



High-impact innovations for high-salinity membrane desalination

Alexander V. Dudchenko^a, Timothy V. Bartholomew^{b,c}, and Meagan S. Mauter^{d,1} 

^aApplied Energy Division, SLAC National Accelerator Laboratory, Menlo Park, CA 94025; ^bNational Energy Technology Laboratory, Pittsburgh, PA 15236; ^cNETL Support Contractor, Pittsburgh, PA, 15236; and ^dCivil and Environmental Engineering, Stanford University, Stanford, CA 94305

Edited by Manish Kumar, The University of Texas at Austin, Austin, TX, and accepted by Editorial Board Member Pablo G. Debenedetti February 23, 2021 (received for review December 1, 2020)

Reducing the cost of high-salinity (>75 g/L total dissolved solids) brine concentration technology would unlock the potential for vast inland water supplies and promote the safe management of concentrated aqueous waste streams. Impactful innovation will target component performance improvements and cost reductions that yield the highest impact on system costs, but the desalination community lacks methods for quantitatively evaluating the value of innovation or the robustness of technology platforms relative to competing technologies. This work proposes a suite of methods built on process-based cost optimization models that explicitly address the complexities of membrane-separation processes, namely that these processes comprise dozens of nonlinearly interacting components and that innovation can occur in more than one component at a time. We begin by demonstrating the merit of performing simple parametric sensitivity analysis on component performance and cost to guide the selection of materials and manufacturing methods that reduce system costs. A more rigorous implementation of this approach relates improvements in component performance to increases in component costs, helping to further discern high-impact innovation trajectories. The most advanced implementation includes a stochastic simulation of the value of innovation that accounts for both the expected impact of a component innovation on reducing system costs and the potential for improvements in other components. Finally, we apply these methods to identify innovations with the highest probability of substantially reducing the levelized cost of water from emerging membrane processes for high-salinity brine treatment.

innovation | desalination | technoeconomic analysis | cost optimization | osmotically assisted reverse osmosis

The desalination research community has long recognized the need for innovation in high-salinity (>75 g/L total dissolved solids) brine concentration technologies (1), but there is widespread disagreement about optimal technology platforms, little consensus around innovation targets, and few tools to evaluate the impact of research investments. Even research programs focused exclusively on modular, membrane-based brine concentration platforms are highly diverse. Work on high-pressure reverse osmosis (HPRO) seeks to extend the pressure tolerance of reverse osmosis (RO) modules, membranes, and pumps from 85 to 300 bar (2, 3). Other research has focused on process innovations that reduce the retarding osmotic pressure potential, as in osmotically assisted RO (OARO) (4, 5), cascading osmotically mediated RO (6), and low-salt rejection RO (7). Finally, membrane distillation (MD) (8) replaces hydraulic pressure with a vapor pressure driving force, but five decades of technology development has yielded little commercial market penetration (8, 9). While this diversity is valuable early in the technology development life cycle, it has a dilutive and disorienting effect when technologies are not regularly evaluated against one another.

Disparate evaluation metrics are the most significant barrier to performing direct technology comparisons. The academic research community has long used energy efficiency as the preferred metric for evaluating high-salinity desalination technology alternatives (7,

10, 11). In contrast, industrial users primarily evaluate technology options based on the levelized cost of water (LCOW), or the sum of capital expenses (CAPEX) and operating expenses (OPEX) amortized over the lifespan of a desalination plant. Neither community has comprehensively evaluated desalination technology designs as a function of feedwater salinity and desired water recovery or thoroughly considered multiobjective design targets.

While mature RO desalination technology represents both the energy and cost-optimal choice for treating water with <40 g/L total dissolved solids, there is only a weak relationship between energy and cost-optimal designs for most membrane separation platforms. Energy costs at seawater RO facilities account for only ~30% of the LCOW, with the balance stemming from capital expenditures, component replacement, and chemical and labor costs (12, 13). Tradeoffs between capital and operational costs made during system design further complicate this relationship. Cost-optimal RO plant designs use only one or two pressure stages, while an energy-optimal RO plant would be designed with an infinitely large number of membrane stages to minimize energy dissipation (11). This tension between higher capital costs associated with larger membrane areas and higher operating costs associated with lower membrane areas is common to all membrane-based desalination technologies and underscores the importance of evaluating technologies on a single metric. Finally, cost-optimal technology design is a strong function of the size and lifespan of the plant, factors that impact process design but are not represented in minimum energy calculations.

One of the difficulties in aligning the research community around LCOW as the preferred technology evaluation metric is that cost, unlike thermodynamic efficiency, is mutable. Performance

Significance

Researchers lack the tools for quantitatively evaluating the impact of their research on technology costs, especially when those technologies comprise multiple components or when the component costs are highly uncertain. We propose a suite of tools to aid in evaluating technology platforms, setting system- and component-level research targets and identifying high-impact innovation trajectories. These tools are applicable to any technology composed of multiple components whose performance or cost will benefit from innovation, but they are especially valuable for membrane systems in which the high interdependence in components amplifies or dampens the effects of innovation in nonintuitive ways.

Author contributions: A.V.D., T.V.B., and M.S.M. contributed methodology; A.V.D. and T.V.B. contributed formal analysis; and A.V.D. and M.S.M. wrote the paper.

The authors declare no competing interest.

This article is a PNAS Direct Submission. M.K. is a guest editor invited by the Editorial Board.

Published under the [PNAS license](#).

¹To whom correspondence may be addressed. Email: mauter@stanford.edu.

Published September 7, 2021.

improvements in components may reduce system operating costs, while manufacturing innovations may reduce the capital cost of a component (Fig. 1A). The resulting effect on LCOW will depend both on the performance relationships between components in a system and on the relationship of those components to system costs. Membrane systems comprise dozens of tightly coupled components, making it challenging to identify high-impact innovation pathways for reducing the LCOW. Past work has addressed this challenge by performing sensitivity analysis within a process-based cost-optimization modeling framework that recomputes the minimum cost system design and operating condition for each perturbation in component performance or cost. These cost-optimization modeling frameworks have recently been applied to quantify the impact of improved component performance on the LCOW of cost-optimal OARO (4), looping MD (8), and multistage MD (14) designs as a function of feedwater salinity and water recovery.

While single-parameter sensitivity analysis identifies components that substantially impact system LCOW, it provides little practical insight into high-impact innovation trajectories. In

particular, single-component sensitivity analysis ignores the relationship between component performance and component cost (10, 15–19); an ultrahigh-permeability graphene membrane may cost thousands of times more than a conventional polyamide thin-film composite membrane. An isocost curve, visualized in white in Fig. 1A, defines the relationship between component cost and component performance that yields an identical system LCOW. While traversing along the isocost curve will not change the LCOW, component diversification can serve as a valuable lever for altering the balance of capital and operational costs in a system (Fig. 1B). Finally, component innovation strategies with the highest impact on system LCOW will move normal to the isocost curve by targeting increased performance (Fig. 1C, i), reduced cost (Fig. 1C, ii), or a combination thereof (Fig. 1C, iii).

Single-component sensitivity analysis also assumes that the performance of other system components is fixed. In this special case, the value of innovation (VoI), herein defined as the percent change in system LCOW over the percent change in component performance or cost, is constant for each component and easily rank-ordered to identify high-impact innovation investments

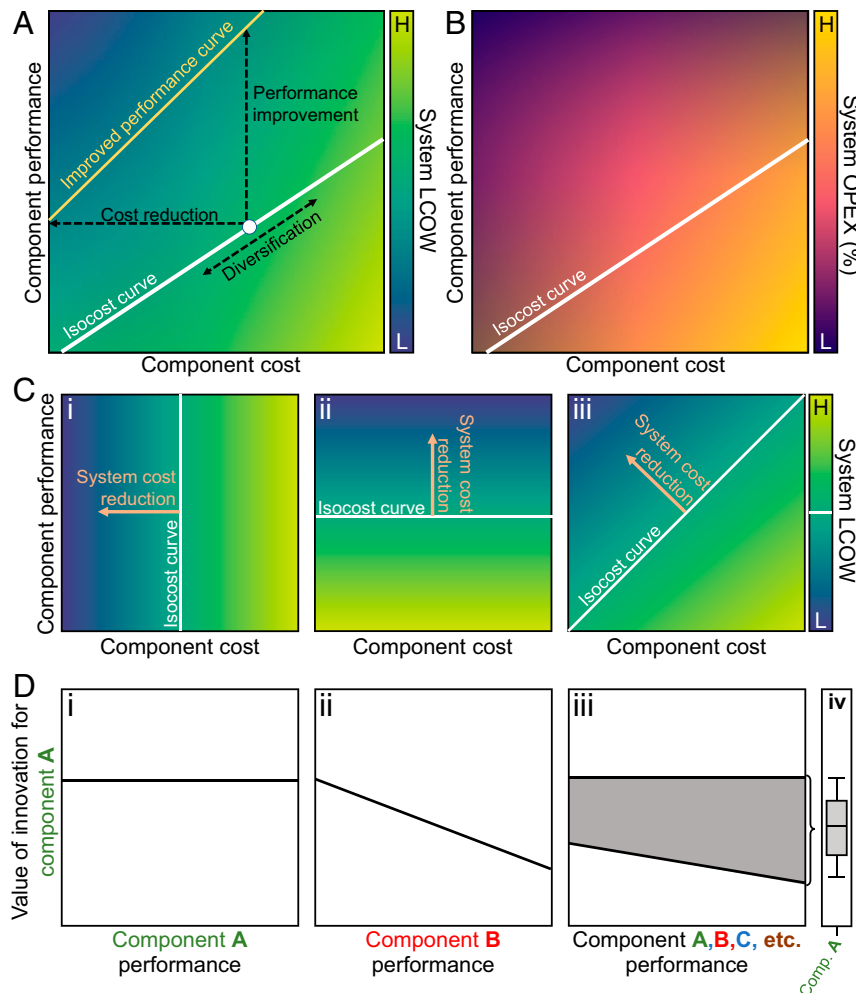


Fig. 1. Methods for identifying critical areas of innovation. (A) The LCOW for a water desalination system depends upon the performance and costs of system components. Decreasing component cost or increasing component performance both reduce the LCOW, so long as the ratio of performance improvement to cost increases is greater than the slope of the isocost curve (white). Component costs are typically expressed in \$ per unit area for membrane module, heaters, etc., or as a complex function of \$ per unit capacity and operation for pumps, pressure exchangers, etc. (B) Innovation along the isocost curve that diversifies the range of available components can provide greater flexibility in the balance of capital expenses (CAPEX) and operational expenses (OPEX), even though the LCOW remains the same. (C) Isocost curves map the relative benefits of component innovations focused on (C, i) reducing costs, (C, ii) increasing performance, or (C, iii) simultaneously reducing costs and increasing performance. Innovation trajectories normal to the isocost curve will provide the most direct route for reducing system cost. (D) The VoI for component A as a function of (D, i) itself, (D, ii) component B, and (D, iii) all system components, which can be summarized in a (D, iv) statistical representation.

(Fig. 1 *D, i*). When innovation occurs simultaneously across multiple components of a coupled system, however, the VoI for any single component depends directly on the performance of all other components (Fig. 1 *D, ii*). Since the shape of the isocost curve differs for each system component, the actual VoI becomes a complex function of the performance and cost of one component relative to other components in the system (Fig. 1 *D, iii*). In these cases, a succinct representation of VoI can only be captured in statistical form, where the VoI with the highest median value and lowest spread identifies the most promising

innovation investment (Fig. 1 *D, iv*). In short, directly accounting for simultaneous and exogenous innovation, or the possibility of innovation spillover from fields, reduces the probability that improvements in other system components render mute innovation investments in the original component of interest. This approach to derisking innovation investments is especially important for systems with large numbers of components.

This paper describes these tools and applies them to identifying high-impact innovation targets for emerging high-salinity brine desalination technologies. We use cost-optimization models

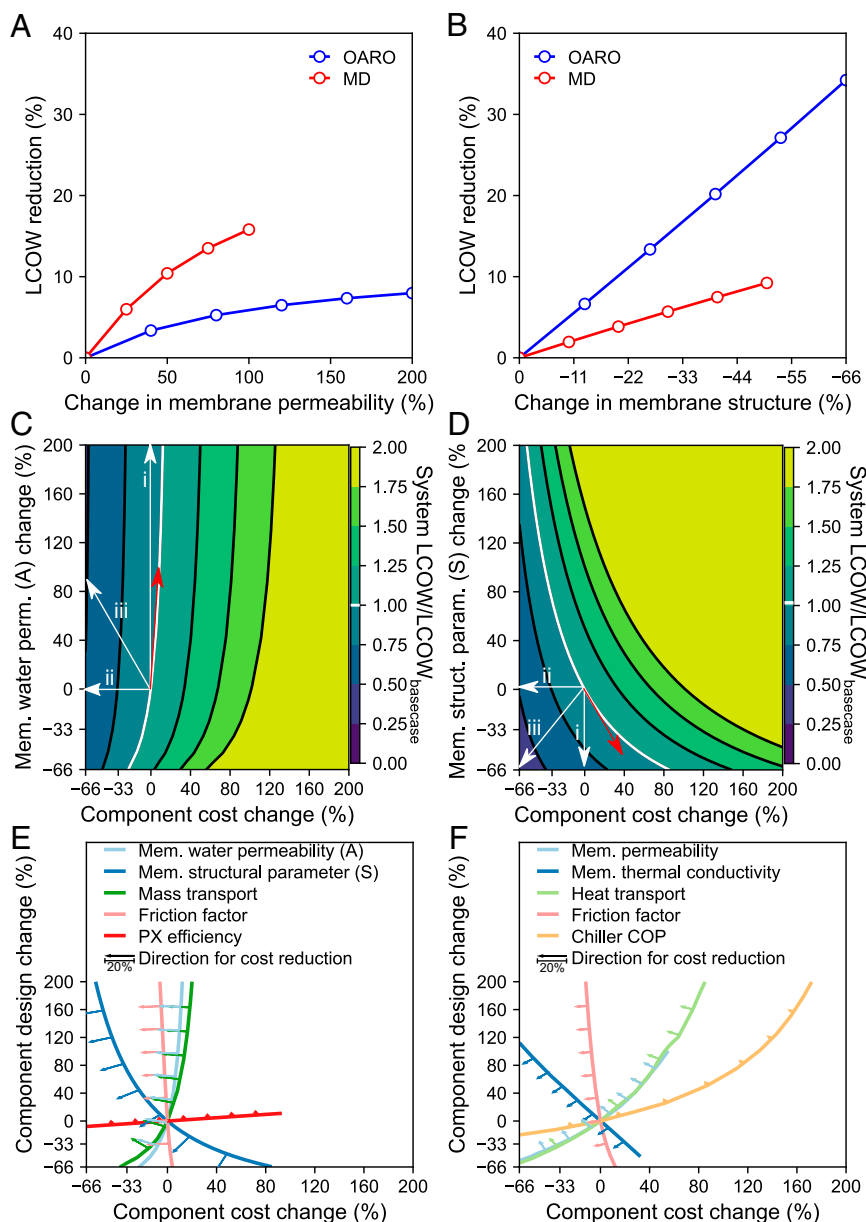


Fig. 2. Sensitivity and isocost analysis for identifying and prioritizing areas of innovation. Traditional sensitivity analysis on (A) membrane permeability and (B) internal mass and energy transport captured in the membrane structural parameter for OARO and the membrane thermal conductivity in MD processes. For MD, the permeability and thermal conductivity are theoretically limited to improvement of 100 and -50% , respectively (details in *Methods, Component Parameters*). Coupled sensitivity analysis of component performance and cost on (C) membrane permeability and (D) structural parameter in OARO process. Performance values for no increase in cost match the results from the traditional sensitivity analysis. In both C and D, arrows (i) represent the direction of performance increase, arrows (ii) represent the direction of cost decrease, and arrows (iii) represent the direction of coupled performance increase and cost decrease. The isocost curves for (E) OARO and (F) MD processes. The lengths of the arrows in E and F indicate the magnitude of system cost reduction. The ranges of PX efficiency, MD permeability, and MD membrane thermal conductivity isocost curves are limited by the theoretical maximum performance as defined in Table 1.

of OARO (4) and multistage MD (14) processes to isolate the effects of component performance improvements on system cost, identify component isocost curves, and stochastically simulate component VoI. Finally, we apply these tools to map the cost-optimal desalination technology landscape for RO, HPRO, OARO, and conductive-gap multistage MD processes as a function of feed salinity, water recovery, and degree of technological innovation. Ultimately, this paper describes both tools and insights for prioritizing high-impact innovation investments in desalination technology.

Results and Discussion

Parametric Sensitivity Analysis. We perform parametric sensitivity analysis to determine how changes in component performance or cost impact the system LCOW. Cost-optimization models are particularly well adapted for parametric sensitivity analysis as they reoptimize process design and operation for each value of component performance or cost to ensure that the processes fully leverage any component improvement (4). Parametric sensitivity analyses of OARO and MD processes suggest that process costs decrease nonlinearly with increased membrane water permeability (Fig. 2A). Similar sensitivity analyses for membrane structural parameters demonstrate that the latter will yield greater reductions in system LCOW (Fig. 2B). Although parametric sensitivity analysis is trivially implemented in most models, the interpretation of results is limited to a single set of component performance or cost parameters.

Performance vs. Cost Innovation. Improving component performance often requires new materials or manufacturing methods that increase component cost, which in turn increase system costs. We propose that coupled performance–cost parametric sensitivity more accurately captures the tradeoffs in component innovation. We perform coupled parametric sensitivity analysis in the OARO cost-optimization model for membrane permeability (Fig. 2C) and the membrane structural parameter (Fig. 2D). The results are presented as a three-dimensional map relating the percent change in component performance and cost to the change in system LCOW (system LCOW/base-case LCOW). This map suggests that increasing membrane water permeability (A) by 100% only reduces system LCOW if the membrane cost increase is less than 10%, while reducing the membrane structural parameter (S) by 50% reduces system LCOW with up to a 40% increase in membrane costs. The most direct route to reduce LCOW is to reduce S and membrane cost simultaneously (arrow *iii* in Fig. 2C and D), although achieving both may be technically challenging.

Isocost curves generalize the results of coupled performance–cost parametric sensitivity analysis by plotting the relationship between performance and cost that yields no change in system costs. In general, the isocost curves are nonlinear and are unique to each component and process. For example, the isocost curve for membrane water permeability (A) in OARO is nearly vertical when costs increase from the base-cost value and has a 45° slope when the costs are below the base-cost value (Fig. 2E). In contrast, the isocost curve for A in MD has a nearly 45° slope across all costs (Fig. 2F).

It is worth noting that the isocost curve does not represent an actual component performance–cost curve. An actual performance–cost curve is a function not only of the manufacturing costs of the component, but also of the retail price that the manufacturer establishes. Manufacturers have an incentive to maximize profits by increasing component prices such that the performance–cost curve mirrors or sits just below the isocost curve. This reality also suggests the need for close collaboration between researchers and industry to differentiate components with high manufacturing costs from components that simply have high prices.

Stochastic Value of Innovation Analysis. As previously discussed, single-component sensitivity analysis assumes that the performance of other system components is fixed. When innovation occurs simultaneously across multiple components of a coupled system, however, the VoI for any single component depends directly on the performance of all other components. The rate of cooccurring innovation is often highly uncertain, which poses challenges for deterministic modeling. Finally, the significant uncertainty in process performance and cost parameters for emerging technologies can also make simple parametric analysis unreliable.

To address these challenges, we propose a method for valuing component innovation under uncertainty (Fig. 3). The proposed stochastic value of innovation analysis (SVoIA) uses a range of possible performance and cost parameters for each component bounded by literature and theory (Fig. 3A, range of values provided in *Methods, Component Parameters*). A random draw from these ranges provides the first reference case, and the cost-optimization model uses these values to calculate a reference system LCOW. Next, the performance and/or cost of the component of interest is improved by a percentile of its full range (Fig. 3B), and the same cost-optimization model is rerun to calculate an improved system LCOW. Finally, the difference between the reference system LCOW and the improved system LCOW is divided by the percentile change to provide the first simulated estimate of VoI. While selecting a percentile change is arbitrary, doing so provides an equivalent basis for comparing VoI across different components. The process is repeated multiple times (1,000 times in this work) to estimate the distribution of possible VoI values for a given component (further details are provided in *Methods, Stochastic Value of Innovation Analysis*).

The SVoIA method can also be used to explicitly account for the unique relationship between cost and performance for each component (Fig. 3B). While the simplest analysis changes cost or performance or both by a fixed percentile, a more complex implementation uses the component-specific performance–cost curve penalty function to determine the change in cost associated with a percentile increase in component performance. The ideal implementation of the SVoIA method would use actual performance–cost curves, but this work overcomes data limitations by using the isocost curve to adjust the component cost. This modification assumes that the isocost curve does not change shape with changes in the performance and cost of other system components, and this assumption is validated if the mean of the stochastically simulated VoI value equals zero.

The VoI for OARO and MD. SVoIA analysis on OARO and MD generates a distribution of VoI values based on a random draw of possible improvements from all system components (Fig. 4). A narrow distribution indicates that the component VoI is not significantly affected by improvements in the component's base value or by improvements in other system components. In contrast, a broad distribution indicates that the VoI for a component is a strong function of improvements in the component itself and other system components. Components with broad VoI should undergo careful parametric analysis to identify which components diminish the VoI before identifying whether the innovations in the given component can significantly reduce cost. The component with the highest positive median and narrowest distribution of VoI is an ideal area for innovation investment.

The simplest SVoIA analysis simulates improvements in component performance under the naive assumption that component performance is independent of cost (Fig. 4, red). For example, in OARO, we find that increasing the membrane structural parameter and the maximum operating pressure will consistently reduce system cost regardless of improvements in

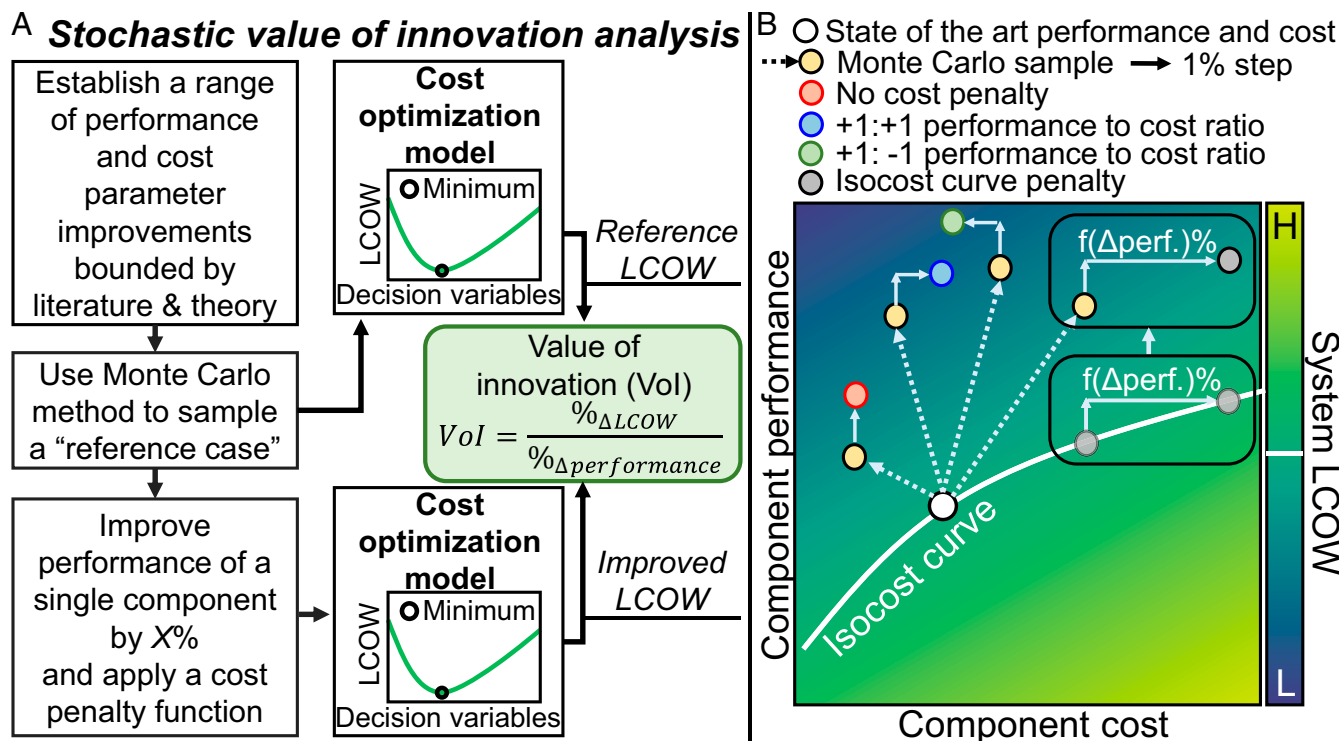


Fig. 3. (A) SVoIA. The method estimates a statistical distribution of the value of innovation for a single component under uncertainty stemming from simultaneous innovations in coupled components. The range of performance and cost parameters is bounded by values from theory and literature. Each Monte Carlo step generates a new reference case that is solved with a cost-optimization model to produce a reference LCOW. The metrics for individual components are adjusted individually and solved with the same cost-optimization model to generate an improved LCOW. The value of innovation is calculated by dividing the change in LCOW by the percentile change in component performance. These steps are repeated 1,000 times to generate a representative distribution of possible values. (B) Four methods of coupling performance change to cost in the SVoIA method. Ideally, an actual cost–performance curve based on real component performance and pricing data would replace the isocost curve in the SVoIA analysis.

other system components. In contrast, innovations in membrane permeability have a broad VoI distribution, with a very low median and a lower-quartile range of values approaching zero. These results suggest that improvements in other components could significantly erode the value of increased membrane permeability in reducing system LCOW. The VoI values for MD systems tend to have a narrower distribution, suggesting that innovations that increase heat transport and membrane permeability and decrease thermal conductivity will reduce system costs even as other system components improve.

More thorough SVoIA analyses account for the effects of changing component performance on component cost. We explore three performance-to-cost ratios: +1:+1 (blue), +1:-1 (green), and +1:X, where X is determined by the isocost curve (gray). We find that the +1:+1 performance-to-cost ratio yields a negative VoI for almost all components across both OARO and MD processes. Only improving the membrane structural parameter and maximum operating pressure in OARO resulted in a positive VoI. Conversely, increasing performance and decreasing cost in a +1:-1 ratio resulted in a positive VoI for all components. While both of these performance-to-cost ratios are arbitrary, the difference between the blue and green cases quantifies the sensitivity of the given component to cost changes. Results for OARO and MD suggest that decreasing the component costs will result in a higher reduction in system costs than that which would be accomplished by increasing component performance.

As previously mentioned, the SVoIA method would ideally use actual performance–cost curves for each component to precisely quantify the VoI. Unfortunately, these curves are often unavailable because the technology is emerging or the manufacturing cost data are uncertain. Here, we use the slope of

component-specific isocost curves as a model for how complex cost–performance relationships affect the VoI. This analysis is also interesting because the SVoIA tests the generalizability of the isocost curves beyond the base-case parameter values on the basis of which they are developed. If the cost ratio is derived from a generalizable isocost curve, the VoI should be zero because any performance gain should be nullified by an increase in component cost. Cases in which the VoI is nonzero indicate that the isocost curve shifts as other components and system specifications change.

Most components have a zero or negative VoI when the slope of the isocost curve is used to inform the performance-to-cost ratio in OARO and MD (Fig. 4, gray). A zero VoI indicates that the isocost curve is accurate across all tested component performance and cost values, and these isocost curves can be used to define the maximum tolerable cost increase with a performance increase. A negative VoI indicates that improving other system components reduces the marginal benefit of improving the performance of the component of interest, while a marginal increase in cost results in a higher increase in system costs. In short, a negative VoI indicates that the isocost curve should be reevaluated when other system components or costs change.

Applications and Conclusions

This work describes and applies three distinct approaches for estimating the value of innovation. While these methods are generalizable to any technology, they are particularly valuable for assessing the value of innovation in technologies whose overall performance and cost are a complex function of multiple components and/or emerging technologies where there is significant uncertainty in the future cost or performance values of each

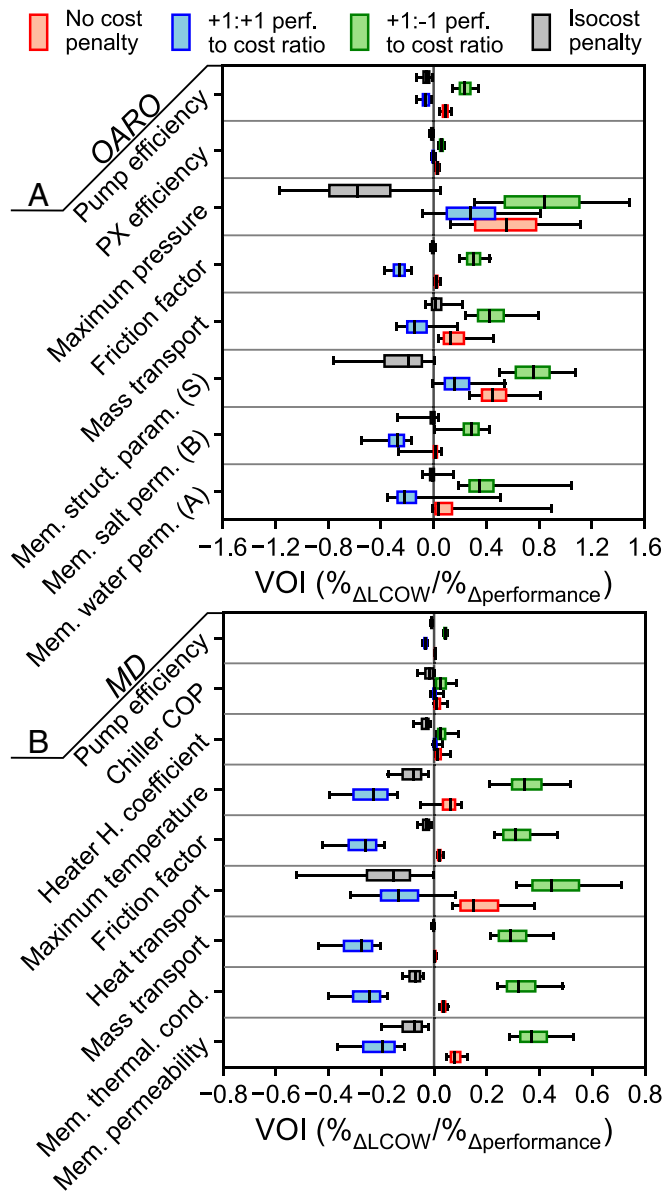


Fig. 4. Value of innovation for OARO and MD. VoI for components in (A) OARO and (B) MD processes. Positive VoI indicates system LCOW reduction. Negative VoI indicates system LCOW increase. The box plots show the median and the 25th and 75th percentile range, while whiskers represent lower and upper inner-quartile range times 1.5.

component as a result of simultaneous innovation across multiple components of a system. While simple parametric analysis within a cost-optimization framework can be used to guide component selection, we demonstrate that coupled performance–cost parametric sensitivity analysis in a cost-optimization framework is essential for quantifying the effects of component innovation on system LCOW. We also demonstrate how coupled performance–cost sensitivity analysis and the resulting isocost maps can guide researchers in pursuit of the most direct routes to system LCOW reductions by focusing innovation on either component performance improvements or component cost reductions. Finally, we present and apply SVoIA as a case-independent and robust approach to providing a distribution of VoI values for a component. The results of parametric analysis and SVoIA clearly demonstrate that increases in component costs can significantly reduce the VoI for a given component, highlighting the need for careful consideration of when

to adopt exotic materials or complex manufacturing methods in pursuit of improved component performance.

The power of cost-optimization models extends beyond simply identifying critical areas of innovation. They also provide a mechanism for evaluating whether an emerging technology offers value within the current technology landscape and how robust that value proposition is to innovations in other technologies. Here, for example, we apply these cost optimization models to estimate the LCOW of OARO and MD processes across a broad range of water recoveries and feed salinities using performance and cost data for state-of-the-art components (Fig. 5A). The cost-optimal water desalination technology for a 50% water recovery target switches from RO at 50 g/L to OARO and to MD at 125 g/L NaCl feed. We found that increasing the performance of all system components by 50% and reducing the cost of all system components by 50% in OARO and MD reduced the treatment costs to below $4 \text{ \\$}/\text{m}^3$ and slightly shifted the transition point from OARO to MD to 150 g/L of NaCl feed (Fig. 5B). It did not, however, eliminate the benefits of switching desalination technology platforms as feedwater salinity increased.

We further extend this analysis to include a hypothetical technology case of HPRO operating at up to 300 bar applied pressure, a pressure range that past work has demonstrated would significantly reduce the cost and energy intensity of high-salinity brine desalination (2). Extending the pressure tolerance of RO modules above 85 bar will require significant innovation in modules (and subcomponents such as membranes, permeate spacers, etc.), pumps, and pressure exchangers. We use a simple multistage HPRO model and apply a cost-escalation function that is a linear function of applied pressure between 85 and 300 bar and the HPRO cost multiplier, evaluated parametrically from 1 to 10. We compare HPRO costs with state-of-the-art and ideal MD and OARO processes as a function of the HPRO cost multiplier and salinity at 50% water recovery (Fig. 5C). We find that HPRO provides a lower system LCOW than does OARO for the full HPRO cost multiplier range explored here and provides a lower LCOW than does MD for HPRO cost multipliers below 7. Because we also expect innovation in OARO and MD system components, we also plot the transition point for ideal OARO and MD from Fig. 5B. The significant decrease in the permissible HPRO cost multiplier for the ideal OARO and MD cases underscores the importance of accounting for potentially simultaneous innovations that benefit competing technology platforms. One logical component performance to account for in OARO would be higher pressure modules, as the component innovations that are likely to enable HPRO are also likely to spill over into performance improvements for OARO.

Whenever performing technology evaluation or VoI analysis, it is also important to account for nontechnological factors that influence system adoption. While it is impossible to comprehensively evaluate all possible factors for each industry seeking more cost-effective high-salinity brine treatment, the ratio of operational to capital expenses is an exogenous decision factor common to most projects. Innovations that expand the range of possible OPEX to CAPEX ratios through component diversification (Fig. 1A) can facilitate adoption of emerging technologies even without changing the LCOW. We apply coupled performance–cost parametric analysis in OARO, finding that innovations that change pump efficiency and cost can alter OPEX by 6% while retaining the same system LCOW (Fig. 5D). Manipulating the performance and cost of all system components could allow even larger adjustment in the OPEX/CAPEX balance. While diversification of component performance and cost is germane to consumer products, efforts to value innovation would benefit from exploring this or other exogenous factors explicitly.

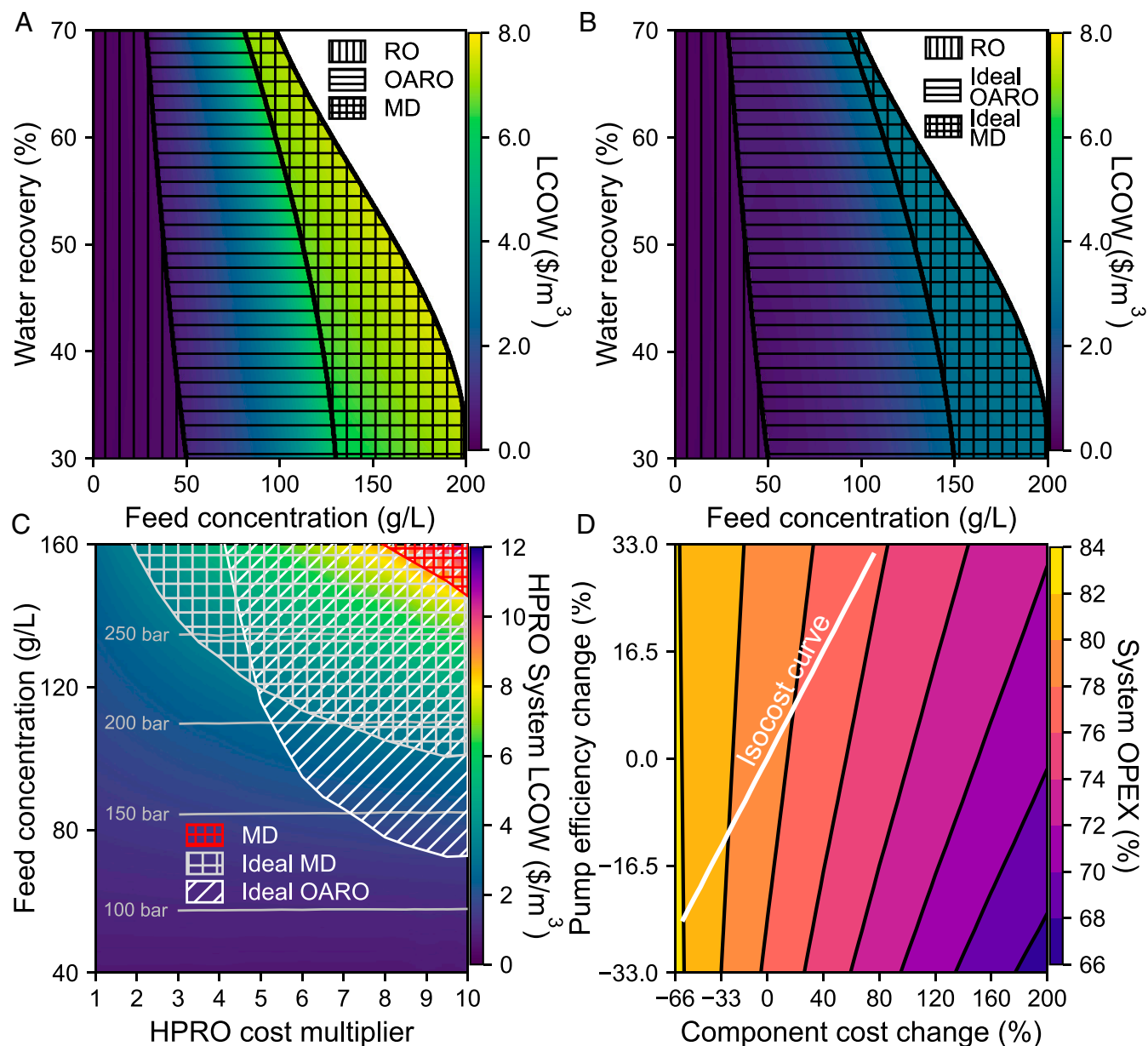


Fig. 5. Application of cost-optimization models for assessing the competitiveness of technology platforms and setting innovation targets. A technology map identifies the lowest-cost technology and associated LCOW for a range of feed concentrations and water recoveries. (A) Technology map for current cost-optimal designs of RO, OARO, and MD, where model parameters are provided in previously published work (4, 14) and restated in Table 1. (B) Technology map for ideal OARO and MD cost-optimal designs, where the “ideal” parameter values increase component performance by 50% and decrease component cost by 50%. (C) Cost estimate of multistage HPRO process with 50% recovery operating at up to 300 bar as a function of feed salinity and the component cost multiplier. The cost-multiplier approach is fully detailed in *Methods*. Gray lines demarcate the operating pressure required to achieve the specified 50% water recovery. Shaded regions indicate where competing technologies would provide a lower LCOW than would HPRO. (D) Percentage of operational expenses (OPEX) to total costs for OARO as a function of change in pump efficiency and cost. White line represents the isocost curve for pump efficiency.

Methods

Cost-Optimization Models. We use previously presented cost-optimization models of OARO, multistage MD, and multistage RO (4, 14, 20). Briefly, the cost-optimization models discretize mass and heat transport in module flow channels along the fluid-flow direction. For OARO and MD, only the counterflow operation is considered. In all processes, concentration and thermal polarization are modeled using traditional thin-film theory, and mass and heat transport rates are estimated from Sherwood and Nusselt correlations. Models consider the effect of salinity and temperature on water density, viscosity, vapor pressure, enthalpy of vaporization, and heat capacity. The models find cost-optimal equipment sizes (membrane area, pump sizes, heater sizes, pressure exchanger size, etc.) and operating conditions

(operating pressure, flowrates, temperatures, heating duty, etc.) for a given feedwater salinity and water recovery. For multistage processes, the optimal number of stages is found by iteratively solving the model with an increasing number of stages until the minimum LCOW is identified. Details on the process and financial parameters are described in our previous work (4, 8, 14, 20).

The HPRO model uses the multistage RO cost-optimization model with additional modifications (20). First, we allow the operating pressure to reach 300 bar. Second, we use an additional RO stage to treat the permeate if the HPRO permeate quality exceeds 0.5 g/L of NaCl. We account for the additional waste stream when calculating the overall water recovery. Third, we model the capital cost of the HPRO equipment (membrane module, pumps, and pressure exchangers) ($CC_{\text{hpro-equipment}}$) as a function of operating

pressure as shown in Eq. 1, where $CC_{ro-equipment}$ is the capital cost of RO equipment, CM is the cost multiplier, and P_{op} is the operating pressure.

$$CC_{hpro-equipment} = CC_{ro-equipment} \times CM(P_{op}). \quad [1]$$

CM is determined from Eq. 2 and is based on a modified softplus activation function, where P_s is the standard RO module pressure of 85 bar and c_s is the cost-function slope found from Eq. 3. This function has a value of 1 between 0 and 84 bar; between 84 and 86 bar, the function smoothly transitions to a linear function that monotonously increases to the specified multiplier at 300 bar.

$$CM = \log(1 + e^{P_{op}-P_s}) \times c_s + 1 \quad [2]$$

The c_s value is found using Eq. 3 for the desired CM at a maximum operating pressure of 300 bar.

$$c_s = (CM - 1) / \log(1 + e^{300-P_s}) \quad [3]$$

The membranes in HPRO models use the standard A parameter of 4.2×10^{-12} m/Pa-s and B parameter of 3.5×10^{-8} m/s for RO membranes (4). This is likely to be a highly optimistic assumption for polymeric membrane materials, but we lack good models for estimating the effects of pressure on A and B parameters.

Component Parameters. We use previously identified state-of-the-art performance and cost parameters for base values (Table 1). The base performance and cost values are used in all of the parametric analyses and serve as a lower bound for SVoIA analysis. The upper bounds on the improved values are based on prior theoretical analyses, literature values, and optimistic approximations based on the current state of the art.

We assume that the upper bounds for improved membrane performance parameters for OARO are based on prior reports of the achieved performance in RO and pressure-retarded osmosis using novel membrane structures, materials, and synthesis methods (16, 21, 22). The upper bounds for improved MD water-vapor permeability and thermal conductivity are based on the theoretical limitation of water-vapor transport and heat transport in a membrane with infinite porosity and pore size in an ambient environment (23–25).

We base our assumptions for the upper bound of the improved values of mass transport, heat transport, and friction factor on the finding that spacer design can be readily adjusted to increase convection or reduce the friction factor by 3x through the simple adjustment of the spacer hydraulic diameter (e.g., fiber diameter, spacing, and angle) (26). More recent methods that use

advanced manufacturing techniques may provide further increases in mass and heat transport without increasing the pressure drop in the module (27).

We crudely estimate the improved maximum operating pressure for OARO as 100 bar from a modest decrease in the current highest-pressure RO module created by DuPont that is rated to operate at 125 bar. We select the maximum temperature in MD based on the fact that operation at 99 °C may not require changes in module designs, as most plastics can operate in this range when at the low pressure typical of MD.

We set the upper bound for improved performance of pressure exchangers on the current state-of-the-art isobaric devices that achieve pressure recovery of up to 97%, making it likely that efficiency of 99% is achievable (28). Similarly, pump efficiency is based on commonly reported values ranging between 75 and 90%, with further innovations potentially pushing efficiency to 95% (29). The upper bound of the chiller coefficient of performance (COP) is based on typical values reported for evaporative cooling towers at power plants, which could be optimized for use in MD process operation (30).

In each case, these upper-bound performance parameters are subject to practical challenges associated with manufacturing sophisticated components at scale. Showstoppers such as the need for extraordinarily high materials purity or the infeasibility of manufacturing a component at scale could either shift these upper bounds back toward state-of-the-art values or significantly lengthen the component development process (31). This not only increases component development costs, but also raises the possibility that a viable approach is abandoned because it becomes obsolete in the face of other component innovations or it becomes anchored in the trough of disillusionment and is abandoned even when manufacturing innovations make it feasible.

Component manufacturers often have the best insight into the limitations of and opportunities for component cost reductions. Lacking this proprietary knowledge, we estimate the maximum potential cost reduction for most components to be 66% or 3x lower than the base cost. The exception is membrane modules, for which we have better cost data. We assume OARO module costs reduce to 30 \$/m², matching the costs of RO modules (4). For MD, we assume the cost can be reduced from 200 to 60 \$/m², which is double the RO module costs due to the use of a gap-module design that includes three flow channels and a metal condensing plate (8). In the sensitivity analysis, we assume that a change in membrane module subcomponent cost (e.g., membrane, spacer, housing, etc.) affects the cost of all subcomponents equally. We make this simplification to avoid assumptions about the cost breakdown of subcomponents in the module.

Finally, we include variation in energy and steam cost, based on typical values for industrial processes (4, 30, 32). This range captures variation in

Table 1. Base and improved values used in cost-optimization models and for SVoIA analysis

Device level	Design parameters	OARO			MD		
		Base values	Improved values	Unit	Base values	Improved values	Unit
Module	Membrane permeability	1×10^{-12}	1×10^{-11}	m/Pa-s	1.5×10^{-10}	2.5×10^{-10}	kg/m-s-Pa
	Salt permeability	8×10^{-8}	1×10^{-8}	m/s			
	Structural parameter	1,200	300	μm			
	Thermal conductivity				0.05	0.025	W/mK
	Mass transport	0	200	% _{adj}			
	Heat transport				0	200	% _{adj}
	Friction factor	0	-66	% _{adj}	0	-66	% _{adj}
	Maximum pressure	65	100	bar			
	Maximum temperature				90	99	°C
	Module cost	50	30	\$/m ²	200	60	\$/m ²
Energy transfer devices	PX efficiency	90	99	%			
	PX cost	0	200	% _{adj}			
	Heater heat transfer coefficient				0	200	% _{adj}
	Heater cost				0	-66	% _{adj}
Pumps	Chiller COP				7	21	COP
	Chiller cost				200	60	\$/kW
	Pump efficiency	75	95	%	75	95	%
Energy cost	Pump cost	0	-66	% _{adj}	0	-66	% _{adj}
	Steam cost				9	3	\$/ton
	Electrical energy cost	0.08	0.02	\$/kWh	0.08	0.02	\$/kWh

The unit of %_{adj} identifies those performance and cost relationships that are based on functions rather than on a single value (i.e., Sherwood correlation) and are increased or decreased by the %_{adj} value, where zero does not change the performance or cost metric.

local energy costs within the SVoIA method but is not considered to be an area for potential innovation due to the maturity of industrial heating processes.

Stochastic Value of Innovation Analysis. The SVoIA analysis is performed as described in *Results and Discussion*. The Vol is found from Eq. 4, where $\%_{\Delta LCOW}$ is found from Eq. 5, $LCOW_{reference}$ is the process cost found for the reference case, and $LCOW_{improved}$ is the system cost found for the improved case.

$$Vol = \frac{\%_{\Delta LCOW}}{\%_{\Delta performance}}, \quad [4]$$

$$\%_{\Delta LCOW} = \frac{LCOW_{improved} - LCOW_{reference}}{LCOW_{reference}} \times 100\%. \quad [5]$$

We use single percentile steps ($\%_{\Delta performance} = 1$) to improve performance or cost as defined by Eq. 6, rather than a percent increase from the base value.

$$Perturbed\ value = |improved\ value - base\ value| \times \frac{\%_{\Delta performance}}{100} + base\ value. \quad [6]$$

For the isocost penalty method, the points along the isocost curves were extracted directly from the coupled parametric sensitivity analysis for each

component, and interpolation was used in the SVoIA analysis to calculate the change in cost with a change in component performance.

Data Availability. All study data are included in the article.

ACKNOWLEDGMENTS. This material is based upon work supported by the National Alliance for Water Innovation, funded by the US Department of Energy, Office of Energy Efficiency and Renewable Energy, Advanced Manufacturing Office, under Funding Opportunity Announcement DE-FOA-0001905. This project was funded by the Department of Energy, National Energy Technology Laboratory, an agency of the United States Government, through a support contract. Neither the United States Government nor any agency thereof, nor any of its employees, nor the support contractor, nor any of their employees, makes any warranty, express or implied, or assumes any legal liability or responsibility for the accuracy, completeness, or usefulness of any information, apparatus, product, or process disclosed, or represents that its use would not infringe privately owned rights. Reference herein to any specific commercial product, process, or service by trade name, trademark, manufacturer, or otherwise does not necessarily constitute or imply its endorsement, recommendation, or favoring by the United States Government or any agency thereof. The views and opinions of the authors expressed herein do not necessarily state or reflect those of the United States Government or any agency thereof.

- M. S. Mauter, P. S. Fiske, Desalination for a circular water economy. *Energy Environ. Sci.* **13**, 3180–3184 (2020).
- D. M. Davenport, A. Deshmukh, J. R. Werber, M. Elimelech, High-pressure reverse osmosis for energy-efficient hypersaline brine desalination: Current status, design considerations, and research needs. *Environ. Sci. Technol. Lett.* **5**, 467–475 (2018).
- D. M. Davenport et al., Thin film composite membrane compaction in high-pressure reverse osmosis. *J. Membr. Sci.* **610**, 118268 (2020).
- T. V. Bartholomew, N. S. Siefert, M. S. Mauter, Cost optimization of osmotically assisted reverse osmosis. *Environ. Sci. Technol.* **52**, 11813–11821 (2018).
- T. V. Bartholomew, L. Mey, J. T. Arena, N. S. Siefert, M. S. Mauter, Osmotically assisted reverse osmosis for high salinity brine treatment. *Desalination* **421**, 3–11 (2017).
- X. Chen, N. Y. Yip, Unlocking high-salinity desalination with cascading osmotically mediated reverse osmosis: Energy and operating pressure analysis. *Environ. Sci. Technol.* **52**, 2242–2250 (2018).
- Z. Wang, A. Deshmukh, Y. Du, M. Elimelech, Minimal and zero liquid discharge with reverse osmosis using low-salt-rejection membranes. *Water Res.* **170**, 115317 (2020).
- T. V. Bartholomew, A. V. Dudchenko, N. S. Siefert, M. S. Mauter, Cost optimization of high recovery single stage gap membrane distillation. *J. Membr. Sci.* **611**, 118370 (2020).
- N. Thomas, M. O. Mavukkandy, S. Loutatidou, H. A. Arafat, Membrane distillation research & implementation: Lessons from the past five decades. *Separ. Purif. Tech.* **189**, 108–127 (2017).
- M. Elimelech, W. A. Phillip, The future of seawater desalination: Energy, technology, and the environment. *Science* **333**, 712–717 (2011).
- S. Lin, M. Elimelech, Staged reverse osmosis operation: Configurations, energy efficiency, and application potential. *Desalination* **366**, 9–14 (2015).
- D. Akgul, M. Çakmakçı, N. Kayaalp, I. Koyuncu, Cost analysis of seawater desalination with reverse osmosis in Turkey. *Desalination* **220**, 123–131 (2008).
- N. Ghaffour, T. M. Missimer, G. L. Amy, Technical review and evaluation of the economics of water desalination: Current and future challenges for better water supply sustainability. *Desalination* **309**, 197–207 (2013).
- A. Dudchenko, T. V. Bartholomew, M. Mauter, Cost optimization of multi-stage gap membrane distillation. *J. Membr. Sci.*, in press.
- D. M. Stevens, J. Y. Shu, M. Reichert, A. Roy, Next-generation nanoporous materials: Progress and prospects for reverse osmosis and nanofiltration. *Ind. Eng. Chem. Res.* **56**, 10526–10551 (2017).
- M. G. Shin et al., Facile performance enhancement of reverse osmosis membranes via solvent activation with benzyl alcohol. *J. Membr. Sci.* **578**, 220–229 (2019).
- C. Su et al., Novel three-dimensional superhydrophobic and strength-enhanced electrospun membranes for long-term membrane distillation. *Separ. Purif. Tech.* **178**, 279–287 (2017).
- M. E. Leitch, C. Li, O. Ikkala, M. S. Mauter, G. V. Lowry, Bacterial nanocellulose aerogel membranes: Novel high-porosity materials for membrane distillation. *Environ. Sci. Technol. Lett.* **3**, 85–91 (2016).
- Z.-X. Low et al., Perspective on 3D printing of separation membranes and comparison to related unconventional fabrication techniques. *J. Membr. Sci.* **523**, 596–613 (2017).
- X. Liu, S. Shanhag, T. V. Bartholomew, J. F. Whitacre, M. S. Mauter, Cost comparison of capacitive deionization and reverse osmosis for brackish water desalination. *ACS EST Engg.* **1**, 261–273 (2020).
- S. Sahebi et al., Developing novel thin film composite membrane on a permeate spacer backing fabric for forward osmosis. *Chem. Eng. Res. Des.* **160**, 326–334 (2020).
- C. F. Wan, T. Yang, W. Gai, Y. D. Lee, T.-S. Chung, Thin-film composite hollow fiber membrane with inorganic salt additives for high mechanical strength and high power density for pressure-retarded osmosis. *J. Membr. Sci.* **555**, 388–397 (2018).
- A. V. Dudchenko et al., Impact of module design on heat transfer in membrane distillation. *J. Membr. Sci.* **601**, 117898 (2020).
- M. E. Leitch, G. V. Lowry, M. S. Mauter, Characterizing convective heat transfer coefficients in membrane distillation cassettes. *J. Membr. Sci.* **538**, 108–121 (2017).
- S. G. S. Beirão, A. P. C. Ribeiro, M. J. V. Lourenço, F. J. V. Santos, C. A. Nieto de Castro, Thermal conductivity of humid air. *Int. J. Thermophys.* **33**, 1686–1703 (2012).
- A. R. Da Costa, A. G. Fane, D. E. Wiley, Spacer characterization and pressure drop modelling in spacer-filled channels for ultrafiltration. *J. Membr. Sci.* **87**, 79–98 (1994).
- N. Thomas et al., 3D printed triply periodic minimal surfaces as spacers for enhanced heat and mass transfer in membrane distillation. *Desalination* **443**, 256–271 (2018).
- R. L. Stover, Seawater reverse osmosis with isobaric energy recovery devices. *Desalination* **203**, 168–175 (2007).
- V. K. Arun Shankar, S. Umashankar, S. Paramasivam, N. Hanigovszki, A comprehensive review on energy efficiency enhancement initiatives in centrifugal pumping system. *Appl. Energy* **181**, 495–513 (2016).
- A. Carrero-Parreño et al., Optimization of multistage membrane distillation system for treating shale gas produced water. *Desalination* **460**, 15–27 (2019).
- K. S. Walton, D. S. Sholl, Research challenges in avoiding, “Showstoppers” in developing materials for large-scale energy applications. *Joule* **1**, 208–211 (2017).
- S. Tavakkoli, O. R. Lokare, R. D. Vidic, V. Khanna, A techno-economic assessment of membrane distillation for treatment of Marcellus shale produced water. *Desalination* **416**, 24–34 (2017).